# scientific reports

OPEN

# Fossil and non-fossil sources of the carbonaceous component of PM$_{2.5}$ in forest and urban areas

Ji-Yeon Cha[1], Kyuyeon Lee[1], Seung-Cheol Lee[1], Eun-Ju Lee[2], Kwang-Jin Yim[3], Ilhan Ryoo[4], Minhye Kim[4], Jinho Ahn[3], Seung-Muk Yi[4,5], Chan-Ryul Park[6] & Neung-Hwan Oh[1,2✉]

Atmospheric particulate matter (PM$_{2.5}$) can damage human health. Biogenic organic compounds emitted from trees may increase the concentration of PM$_{2.5}$ via formation of secondary aerosols. Therefore, the role of biogenic emissions in PM$_{2.5}$ formation and the sources of PM$_{2.5}$ need to be investigated. Dual carbon isotope and levoglucosan analyses are powerful tools to track the sources of total carbon (TC) in PM$_{2.5}$. We collected a total of 47 PM$_{2.5}$ samples from 2019 to 2020 inside a pine forest and in urban areas in South Korea. The average $\delta^{13}C$ and $\Delta^{14}C$ of TC in PM$_{2.5}$ at the Taehwa Research Forest (TRF) were − 25.7 and − 380.7‰, respectively, which were not significantly different from those collected at Seoul National University (SNU) in urban areas. Contribution of fossil fuel, C$_3$-, and C$_4$- plants to carbonaceous component of PM$_{2.5}$ were 52, 27, and 21% at SNU, whereas those were 46, 35, and 19% at TRF, respectively. The biomass burning tracer, levoglucosan, was most abundant in winter and correlated with the contribution of C$_4$ plants derived carbon. Results indicate that biogenic aerosols emitted from trees is less likely to be an important source of PM$_{2.5}$ and that trees can act as a bio-filter to reduce PM$_{2.5}$.

Pollution due to fine particulate matter with a diameter of 2.5 μm or less (PM$_{2.5}$) is a significant challenge, which affects human health and ecosystem, visibility, and climate change[1,2]. The mean annual concentrations of PM$_{2.5}$ ranged from 30.6 to 37.2 μg m$^{-3}$ between 2013 and 2017 in Seoul, the capital of South Korea[3], which still exceed the regulatory standard of 15 μg m$^{-3}$ specified by the Korean government. Higher concentrations of PM$_{2.5}$ are frequently observed[4,5].

Trees can remove atmospheric PM$_{2.5}$ by directly adsorbing PM$_{2.5}$ on the surface of leaves and branches, and by absorbing some of the PM$_{2.5}$ through the stomata[6,7]. The mean annual PM$_{2.5}$ levels removed by trees in the urban areas are estimated at 0.27 and 0.15 g m$^{-2}$ in the conterminous United States and in 86 Canadian cities, respectively[6,8]. In addition, plants alter the local microclimate conditions by reducing air temperature and increasing relative humidity via canopy transpiration, thus increasing the deposition of PM onto leaves[9]. Therefore, this process can reduce the concentration of PM$_{2.5}$ in urban areas[6,9,10]. For example, in central Sydney, Australia, the PM$_{2.5}$ concentrations were lower in urban areas with a relatively higher density of green space[10]. Therefore, urban forest expansion has been regarded as one of the government policies to reduce PM$_{2.5}$ concentrations in many countries[11]. South Korea is no exception, and the Korea Forest Service has proposed an increase in urban green space to 15 m$^2$ per capita from the current 9.9 m$^2$ per capita by 2027[12].

However, trees indirectly increase PM$_{2.5}$ concentrations. Trees emit biogenic volatile organic compounds (BVOCs) such as isoprene and terpenes as well as alcohols, carbonyls, and acids[13]. The oxidation products of these BVOCs can form and grow biogenic secondary organic aerosols (SOAs)[14]. SOAs constitute up to 85% of organic carbon and ∼ 35% of PM$_{2.5}$[15]. SOAs may contribute to the formation of carbonaceous materials in fine particles in the presence of elevated levels of anthropogenic emissions of NOx and oxidants (OH radicals and ozone). For example, the formation of biogenic SOAs can be enhanced by 60–200% due to the emission of NOx and oxidants[16]. The mass concentration of submicron particles is also increased by 25–200% at polluted sites downwind of Manaus, Brazil[17]. Furthermore, studies using radiocarbon ($^{14}C$) reported that a high biogenic

[1]Department of Environmental Planning, Graduate School of Environmental Studies, Seoul National University, Seoul 08826, Republic of Korea. [2]Environmental Planning Institute, Seoul National University, Seoul 08826, Republic of Korea. [3]School of Earth and Environmental Sciences, Seoul National University, Seoul 08826, Republic of Korea. [4]Department of Environmental Health, Graduate School of Public Health, Seoul National University, Seoul 08826, Republic of Korea. [5]Institute of Health and Environment, Seoul National University, Seoul 08826, Republic of Korea. [6]Urban Forests Division, National Institute of Forest Science, Seoul 02455, Republic of Korea. ✉email: onh@snu.ac.kr

fraction can contribute to the formation of carbonaceous component of $PM_{2.5}$ in cities, accounting for up to 80% of the aerosol carbon[18–20].

These findings bring a question on how much biogenic emissions contribute to the formation of $PM_{2.5}$ in the atmosphere and whether the sources of $PM_{2.5}$ in forests are different from urban areas. $^{14}$C is a powerful tracer of the carbon cycle, which separates fossil-fuel-derived carbon from recently photosynthesized carbon. However, the $^{14}$C analysis cannot distinguish if the sources of carbon in $PM_{2.5}$ are generated from biogenic emissions or biomass burning because both are derived from recently photosynthesized carbon[21,22]. Thus, a biomarker is needed to further identify the sources of biogenic $PM_{2.5}$. Levoglucosan has been widely used to trace the pyrolytic emissions of $PM_{2.5}$ released by biomass burning[23–26]. In addition to radiocarbon and levoglucosan analyses, the stable carbon isotope ratio ($\delta^{13}$C) can provide further information on the sources of carbon, *i.e.*, $C_3$ and $C_4$ plants, because of their distinct isotopic fractionation[27,28]. $C_3$ plants (*e.g.*, most trees) incorporate $CO_2$ into the three-carbon compound, 3-phosphoglyceric acid, during the first stage of photosynthesis, whereas $C_4$ plants (*e.g.*, maize and sorghum) initially fix $CO_2$ in the mesophyll cell as a four-carbon compound, oxaloacetate, which results in distinctive $\delta^{13}$C[29,30].

The objectives of this study are (1) to investigate the temporal variation in the concentrations of total carbon (TC) including organic and elemental carbon in $PM_{2.5}$, (2) to compare carbon isotope ratios ($\delta^{13}$C and $\Delta^{14}$C) between a pine forest and urban area, and (3) to track the sources of TC in $PM_{2.5}$ by analyzing $\delta^{13}$C, $\Delta^{14}$C, and levoglucosan concentrations.

## Methods and materials
### Sampling sites and collection of $PM_{2.5}$.
Samples were collected from four sites (Fig. 1a,b) as follows:

1. A Korean pine (*Pinus koraiensis*) forest located at the Taehwa Research Forest (TRF) (37°30.5′N, 127°31.6′E, Fig. 1c), where pines were planted in 1960s[31]. TRF is a part of Seoul National University Forests, and is located in the suburban area[32].
2. The rooftop of a building located in the Seoul National University (SNU) campus (37°45.8′N, 126°95.0′E, Fig. 1d) in the southern part of Seoul (~ 10 million population), the capital of South Korea.
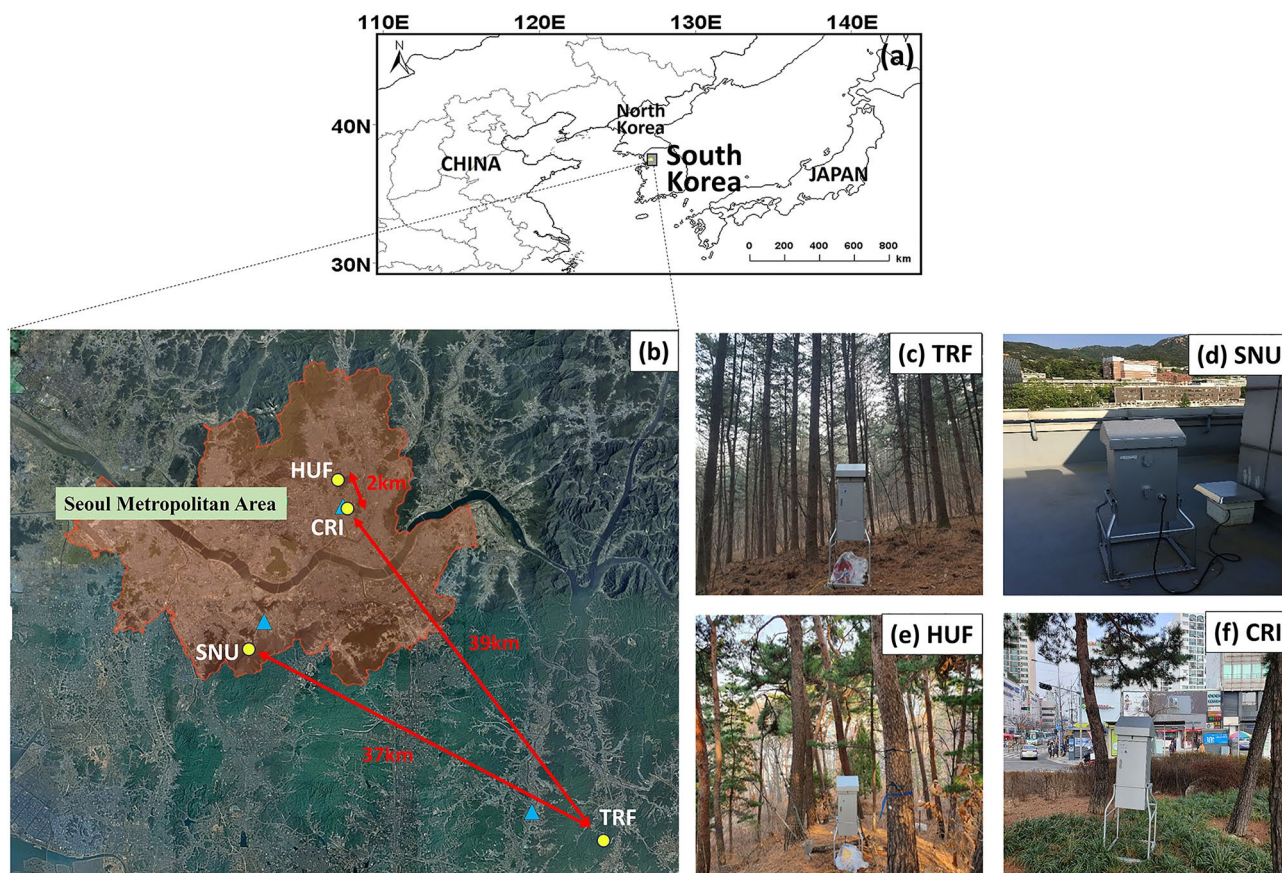


**Figure 1.** (**a**) The location of study sites in South Korea, (**b**) $PM_{2.5}$ sampling points for high-volume air sampler (yellow circles) and the national $PM_{2.5}$ monitoring sites (blue triangles). The high-volume air sampler was set at (**c**) the Taehwa Research Forest (TRF), (**d**) the Seoul National University (SNU), (**e**) the Hongneung urban forest (HUF) and (**f**) Cheongnyangni traffic island (CRI). The map of East Asia in (**a**) was created by MeteoInfo 3.5.5 (http://www.meteothink.org) and the satellite imagery in (**b**) was created on the Vworld platform (http://map.vworld.kr) provided by the Korean Ministry of Land, Infrastructure and Transport.

3.  A pine forest at the Hongneung Urban Forest (HUF) near Mt. Cheonjang (37°59.6′N, 127°04.5′E, Fig. 1e) in Seoul, which is a fragmented forest surrounded by urban residential area. Dominant species include *Pinus densiflora* and *P. koraiensis*.
4.  A green space with pine trees located at Cheongnyangni Traffic Island (CRI) (37°58.0′N, 127°04.5′E, Fig. 1f) in Seoul, which is a small triangle area (0.06 ha) between roads.

According to the Food and Agriculture Organization of the United Nations[33], forest is defined as "land spanning more than 0.5 hectares with trees higher than 5 m and a canopy cover of more than 10 percent, or trees able to reach these thresholds in situ". In that sense, TRF is a pine forest in rural area. HUF is also a pine forest, but located in urban area. CRI is not a forest but a simple green space with pine trees near busy traffic roads in urban area. SNU is in the urban area. The population size and density are often used to define a place as 'urban'. Seoul is one of the largest metropolitan areas (~ 10 million population) in the world.

A high-volume air sampler (HVAS; HV-1700RW, Sibata, Tokyo, Japan) was used to collect the $PM_{2.5}$ on quartz filters at a flow rate of 1000 L min$^{-1}$[23,28,34,35]. An HVAS was placed on the rooftop of a building at SNU, and the other HVAS was installed inside the forests or green space. The high-volume air samplers were automatically calibrated by a built-in flowmeter, temperature sensor, and atmospheric pressure sensor. No plant parts were sampled in this study. Between 2019 and 2020, a total of 47 samples were collected with a time resolution of 24–72 h (usually 24 h). To collect $PM_{2.5}$ in the atmosphere, the quartz filters were pre-baked at 400 °C for 4 h prior to use for removing the organic contaminants. Quartz filters are widely used to measure carbonaceous aerosols[23,28,34,35] because their composition is carbon-free, and can remain stable at temperatures up to 900 °C for carbon isotope analysis. However, the quartz filters were not used to measure the mass of $PM_{2.5}$ because the filter size is too large (203 mm by 254 mm) to be precisely weighed on an analytical balance. Instead, beta attenuation mass monitors (BAM) are widely used to measure the concentration of $PM_{2.5}$ indirectly. Both methods complement each other, BAM for relatively simple estimation of $PM_{2.5}$ concentration and HVAS for isotopic analysis. Similar patterns were observed between $PM_{2.5}$ by BAM and TC in $PM_{2.5}$ by HVAS (Fig. 3a–c), but they were not used for cross-calibration.

Most of the samples were collected at TRF (n = 21) and SNU (n = 18) to compare the sources of carbonaceous component of $PM_{2.5}$ between forest and urban areas (Table 1). A total of 11 samples were simultaneously collected at both TRF and SNU. The additional samples were collected inside the green space or forests at CRI (n = 6) and HUF (n = 2), respectively, in the urban areas during fall and winter (Table 1). After sampling, filters were wrapped in pre-baked aluminum foil and stored at − 20 °C. Field blank filters were also prepared by placing the filter in the sampler for 24 to 72 h without gas flow, and then stored as described above. The mass of carbon on the field blank filters was negligible compared with that of collected $PM_{2.5}$.

**$PM_{2.5}$ monitoring data in South Korea.** The AirKorea website (http://www.airkorea.or.kr) provides nationwide $PM_{2.5}$ data collected from outdoor monitoring sites via β-ray absorption. The method is used to estimate the concentration of $PM_{2.5}$ based on the relationship between attenuation of beta radiation and $PM_{2.5}$ deposited on a glass fiber filter tape within an instrument. We downloaded the daily $PM_{2.5}$ concentration data of the three national monitoring sites (Fig. 1b) from the AirKorea website. One of the monitoring sites for both HUF and CRI was located next to the road, and the monitoring sites for TRF and SNU, respectively, were located at the rooftop of each Community Center. The monitoring site for TRF was located outside the forest, 6.6 km apart from TRF in the rural area, whereas the other monitoring sites were located within 2.4 km of our sampling sites in the urban area. All three national monitoring sites are located outside forests, providing information on $PM_{2.5}$ concentration.

Based on the daily $PM_{2.5}$ data reported by the AirKorea, the sampling dates for HVAS were chosen when the concentration of $PM_{2.5}$ was higher than ~ 15 μg m$^{-3}$, which is the air quality guideline of $PM_{2.5}$. The HVAS was also used in order to collect enough amount of carbon for isotopic analysis which was > ~ 1 mg-C.

**Dual carbon isotope analysis.** The $PM_{2.5}$ samples were acidified with 10% HCl to remove inorganic carbon, and then dried at 50 °C[36–38]. Each dried filter was transferred to a pre-burned quartz tube containing CuO as an oxidant and silver wire. The quartz tube was evacuated, flame-sealed, and heated at 850 °C for 4 h to oxidize total carbon (TC) including organic and elemental carbon. The resulting $CO_2$ in the quartz tube was sent to the national ocean sciences accelerator mass spectrometry facility (https://www2.whoi.edu/site/nosams/) to measure dual carbon isotope ratios ($\delta^{13}C$ and $\Delta^{14}C$) of TC in $PM_{2.5}$ via accelerator mass spectrometry. The IAEA-C8 oxalic acid was routinely used as a reference standard material, and its $\delta^{13}C$ and $^{14}C$ activity was measured within the recommended range (https://nucleus.iaea.org/sites/ReferenceMaterials/Pages/IAEA-C-8.aspx). To our knowledge, this is the first study reporting $\delta^{13}C$ and $\Delta^{14}C$ of $PM_{2.5}$ over an entire year in South Korea.

**Source apportionment of TC in $PM_{2.5}$ using IsoSource and Bayesian statistics.** First, the sources of TC in $PM_{2.5}$ were separated into fossil fuel and non-fossil fuel sources based on radiocarbon results[38]. The contribution of each non-fossil fuel source (i.e., $C_3$ and $C_4$ plants) was further quantified by incorporating the results of stable carbon isotope analysis using IsoSource and Bayesian mixing models. Three endmembers were used: fossil fuel, $C_3$ plants, and $C_4$ plants (Fig. 2). The $\delta^{13}C$ of the three endmembers was set to − 29.0 ± 1.3‰ for fossil fuel, − 26.7 ± 1.8‰ for $C_3$ plants, and − 16.4 ± 1.4‰ for $C_4$ plants[27,39]. The $\Delta^{14}C$ of carbon derived from fossil fuel was set to − 1000‰, while the $\Delta^{14}C$ values of $C_3$ and $C_4$ plants were set to 30‰[36], similar to the $\Delta^{14}C$-$CO_2$ in the troposphere because plants absorb atmospheric $CO_2$ during photosynthesis. Both the $\delta^{13}C$ and $\Delta^{14}C$ results were incorporated to draw quantitative results of carbon sources. The dual isotopic mixing model is commonly used in ecological studies to determine the proportions of various sources in a mixture[28,39,40].

| Date (mm/dd/yyyy) | Collecting period (hours) | TC in PM$_{2.5}$[†] (%) | TC (µg C m$^{-3}$) | δ$^{13}$C (‰) | Δ$^{14}$C (‰) | Levoglucosan (ng m$^{-3}$) | Season |
|---|---|---|---|---|---|---|---|
| Taehwa Research Forest (TRF), Gwangju-si (n = 21) | | | | | | | |
| 08/02/2019 | 24 | 32 | 4.5 | − 26.6 | − 489.9 | NA[‡] | Summer |
| 08/05/2019 | 24 | 19 | 5.3 | − 26.7 | − 250.3 | 6.41 | Summer |
| 01/24/2020 | 24 | 13 | 7.0 | − 25.6 | − 323.0 | NA | Winter |
| 02/07/2020 | 24 | 16 | 5.3 | − 24.5 | − 382.9 | 66.52 | Winter |
| 02/13/2020 | 23 | 10 | 5.3 | − 26.0 | − 441.2 | 44.94 | Winter |
| 02/20/2020 | 24 | 16 | 8.7 | − 26.1 | − 360.2 | 62.92 | Winter |
| 02/21/2020 | 24 | 11 | 6.4 | − 25.5 | − 349.6 | NA | Winter |
| 02/22/2020 | 48 | 9 | 3.5 | − 25.0 | − 357.3 | 60.02 | Winter |
| 04/10/2020 | 24 | 24 | 6.6 | − 23.2 | − 227.8 | 60.47 | Spring |
| 04/13/2020 | 24 | 45 | 4.9 | − 25.0 | − 204.5 | 39.96 | Spring |
| 05/04/2020 | 24 | 35 | 5.6 | − 25.5 | − 273.9 | NA | Spring |
| 05/21/2020 | 24 | 42 | 3.8 | − 26.1 | − 381.8 | 18.94 | Spring |
| 07/08/2020 | 24 | 22 | 3.9 | − 26.3 | − 536.2 | 9.57 | Summer |
| 08/18/2020 | 24 | 15 | 3.4 | − 26.6 | − 576.4 | 8.95 | Summer |
| 09/14/2020 | 24 | 29 | 3.2 | − 25.7 | − 514.0 | 13.98 | Fall |
| 10/13/2020 | 24 | 34 | 4.1 | − 26.0 | − 373.2 | 37.92 | Fall |
| 10/14/2020 | 24 | 29 | 4.3 | − 26.0 | − 311.4 | NA | Fall |
| 10/15/2020 | 24 | 29 | 4.1 | − 26.6 | − 360.3 | NA | Fall |
| 10/16/2020 | 24 | 26 | 4.7 | − 26.8 | − 410.3 | 51.68 | Fall |
| 11/14/2020 | 48 | 7 | 3.0 | − 26.4 | − 375.0 | 34.74 | Fall |
| 12/11/2020 | 24 | 10 | 7.3 | − 24.6 | − 494.9 | 53.08 | Winter |
| Mean | | 22 | 5.0[b] | − 25.7 | − 380.7[b] | 38.01 | |
| Hongneung Urban Forest (HUF), Seoul (n = 2) | | | | | | | |
| 02/20/2020 | 24 | 20 | 8.6 | − 25.7 | − 417.2 | 65.82 | Winter |
| 10/13/2020 | 24 | 49 | 5.4 | − 25.7 | − 370.0 | 40.00 | Fall |
| Mean | | 34 | 7.0[ab] | − 25.7 | − 393.6[ab] | 52.91 | |
| Cheongnyangni Traffic Island (CRI), Seoul (n = 6) | | | | | | | |
| 02/21/2020 | 24 | 17 | 8.2 | − 24.8 | − 433.8 | NA | Winter |
| 02/22/2020 | 48 | 16 | 5.8 | − 25.1 | − 426.4 | 38.46 | Winter |
| 02/24/2020 | 34 | 34 | 6.9 | − 26.0 | − 451.3 | NA | Winter |
| 10/14/2020 | 23 | 66 | 5.4 | − 25.0 | − 421.3 | NA | Fall |
| 10/15/2020 | 24 | 86 | 8.6 | − 25.9 | − 465.6 | NA | Fall |
| 10/16/2020 | 24 | 61 | 10.4 | − 26.0 | − 467.5 | 61.11 | Fall |
| Mean | | 47 | 8.2[ab] | − 25.2 | − 444.3[a] | 49.78 | |
| Seoul National University (SNU) campus, Seoul (n = 18) | | | | | | | |
| 01/14/2019 | 24 | 19 | 25.6 | − 23.7 | 589.7[††] | 4.55 | Winter |
| 02/22/2019 | 24 | 39 | 23.9 | − 23.6 | − 313.7 | 75.91 | Winter |
| 03/05/2019 | 24 | 8 | 10.4 | − 23.7 | − 503.6 | NA | Spring |
| 04/22/2019 | 24 | 28 | 10.0 | − 25.9 | − 239.3 | 9.69 | Spring |
| 05/24/2019 | 24 | 29 | 14.7 | − 26.0 | − 430.1 | NA | Spring |
| 06/05/2019 | 24 | 27 | 9.2 | − 25.8 | − 561.9 | NA | Summer |
| 07/17/2019 | 24 | 14 | 7.4 | − 25.5 | − 370.6 | NA | Summer |
| 08/08/2019 | 24 | 14 | 5.5 | − 26.1 | − 459.4 | 5.57 | Summer |
| 02/07/2020 | 24 | 59 | 16.6 | − 23.6 | − 352.5 | 64.52 | Winter |
| 02/13/2020 | 24 | 12 | 7.0 | − 25.2 | − 370.1 | NA | Winter |
| 04/10/2020 | 24 | 58 | 16.4 | − 22.2 | − 284.9 | 66.24 | Spring |
| 04/13/2020 | 24 | 50 | 7.0 | − 24.1 | − 290.5 | 38.25 | Spring |
| 05/04/2020 | 24 | 69 | 11.0 | − 25.3 | − 400.0 | NA | Spring |
| 05/21/2020 | 24 | 50 | 5.5 | − 26.2 | − 415.6 | 7.41 | Spring |
| 07/08/2020 | 24 | 24 | 5.3 | − 25.7 | − 543.7 | 8.61 | Summer |
| 08/18/2020 | 24 | 12 | 2.8 | − 27.3 | − 635.9 | 4.38 | Summer |
| 09/14/2020 | 24 | 26 | 3.4 | − 26.1 | − 503.6 | 6.63 | Fall |
| 11/13/2020 | 70 | 12 | 5.6 | − 25.3 | − 481.6 | 18.50 | Fall |
| 12/11/2020 | 24 | 16 | 12.3 | − 24.6 | − 439.1 | 70.72 | Winter |
| Mean | | 30 | 9.7[a] | − 25.1 | − 422.0[ab] | 36.36 | |

**Table 1.** Concentrations and key properties of PM$_{2.5}$ collected by high volume air samplers at TRF, HUF, CRI, and SNU. ‡NA: Not assessed. †Calculated by dividing the TC (μg C m$^{-3}$) by the concentration of PM$_{2.5}$ at the national monitoring sites in South Korea near TRF, HUF&CRI, and SNU. ††This extraordinary Δ$^{14}$C sample was excluded from statistical analysis. The details are described in the Supplementary Information.
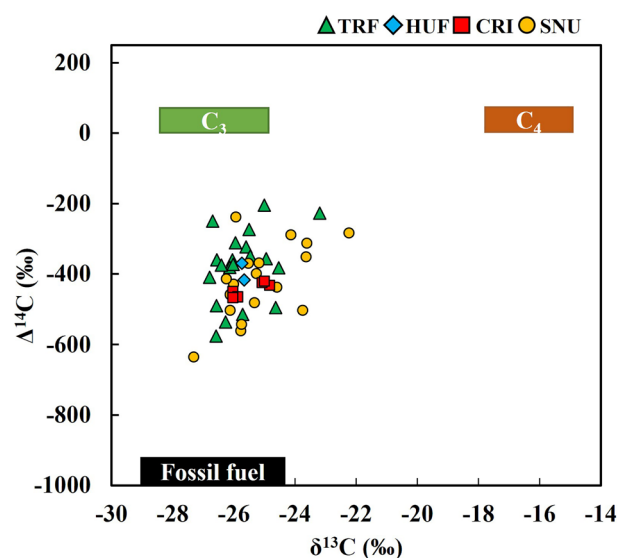


**Figure 2.** Isotopic source diagram for the PM$_{2.5}$ samples. The black, green, and brown bars indicate three endmembers including fossil-, C$_3$ plants-, and C$_4$ plants-derived carbon, respectively.

IsoSource, a popular mixing model, was used to quantify TC in PM$_{2.5}$ sources into fossil fuels, C$_3$ plants, and C$_4$ plants (https://www.epa.gov/eco-research/stable-isotope-mixing-models-estimating-source-proportions)[41]. All possible combinations of source proportions were calculated with IsoSource using a 0.1‰ tolerance. The radiocarbon results were used as additional constraints to further reduce the range of contributions from the fossil fuel sources. The IsoSource results were used as prior information via Bayesian inferences using Markov Chain Monte Carlo (MCMC) method (Figs. S1 and S2 in Supplementary Information). In this MCMC model, the sources were also separated into fossil fuels, C$_3$ plants, and C$_4$ plants. To estimate seasonal source contributions to TC in PM$_{2.5}$, we combined all the data points from each season in the MCMC calculation. Annual source apportionment was conducted by combining all the data points at each site. MCMC was implemented using the *simmr*-0.4.5 (https://cran.r-project.org/web/packages/simmr/index.html) in R-4.1.1[42].

**Levoglucosan analysis.** The dual carbon isotope analysis does not distinguish if the sources of carbon in PM$_{2.5}$ are generated from biogenic emissions or biomass burning. In order to investigate the possibility of the biomass burning as a source of carbon in PM$_{2.5}$, levoglucosan analysis was employed to complement carbon isotope analysis[23–26]. The levoglucosan concentration, which is a biomarker of biomass burning, was analyzed[23–26]. The samples were sonicated with dichloromethane: methanol (3:1, v/v) at 20 °C for 1 h. The extract was concentrated using nitrogen gas in TurbovapII (Zymark Co., USA) and filtered using a 0.45-μm PTFE syringe filter (Pall Corporation, USA). After filtration, the extract was reconcentrated to a final volume of 1 mL using Turbovap II and Reacti-Therm (Thermo Scientific, TS-18822, USA) and stored in a freezer until analysis.

Derivatization via silylation was conducted to analyze polar compounds. A 50 μL aliquot of the final extract volume was completely dried by gently blowing nitrogen gas, followed by reaction with 50 μL of N, O-bis-(trimethylsilyl) trifluoroacetamide (BSTFA) combined with 1% trimethylchlorosilane (TMCS) (Sigma Aldrich, USA) and 50 μL of pyridine (HPLC grade, Sigma Aldrich, USA) at 75 °C for 90 min. After derivatization, the concentration of levoglucosan was determined using a GC/MS (7890B/5977B, Agilent, USA) operating at an ionization energy of 70 eV in EI mode.

**Statistical analysis.** Differences in PM$_{2.5}$ concentrations and carbon isotope signatures among sites and seasons were analyzed via one-way analysis of variance (ANOVA), followed by Tukey's HSD (honest significant difference) test. Type II error (*i.e.*, false negative) can occur when the sample size is too small. The number of samples per season ranged from 2 to 7 in this study, making the statistical analysis on them prone to type II error. Although we fully recognize the limitations of the analysis due to the relatively small number of samples per season, we still have attempted to provide seasonal information of TC in PM$_{2.5}$ as Korea is located in the Asian monsoon climate, where the highest PM$_{2.5}$ concentrations were reported in winter and decreased to a minimum
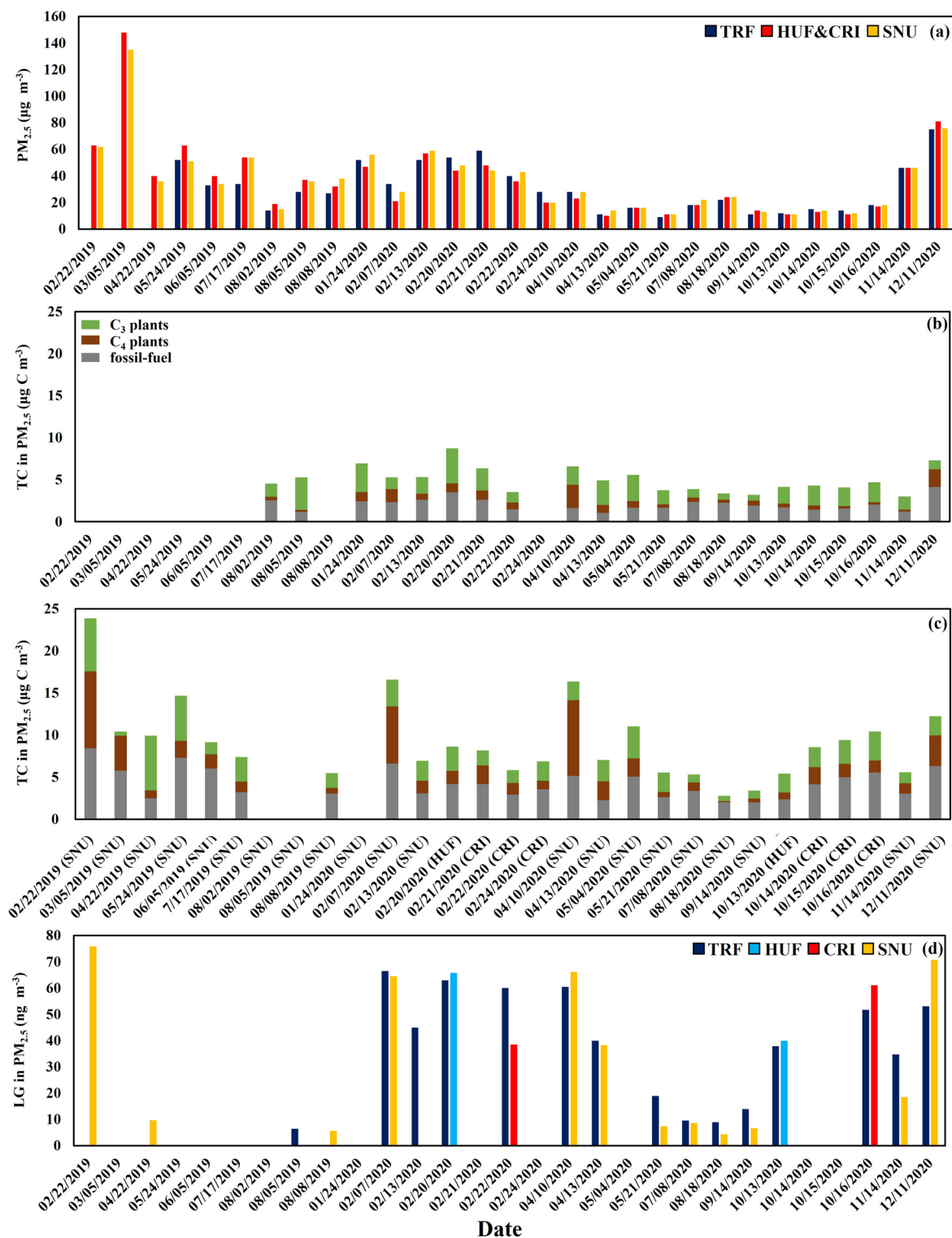
**Figure 3.** (**a**) The concentrations of PM$_{2.5}$ (μg m$^{-3}$) at the national PM$_{2.5}$ monitoring sites near SNU, HUF&CRI (one site; section "PM$_{2.5}$ monitoring data in South Korea"), and TRF. (**b**) The concentration (μg C m$^{-3}$) of TC in PM$_{2.5}$ at TRF. (**c**) The concentrations of TC in PM$_{2.5}$ at SNU, HUF, and CRI. The green, brown, and grey bars in (**b**) and (**c**) represent carbon derived from C$_3$ plants, C$_4$ plants, and fossil fuel, respectively. (**d**) The concentration (ng m$^{-3}$) of levoglucosan.

in summer[3]. A linear regression analysis was used to assess the relationship between levoglucosan concentration and fractional contribution of carbon derived from $C_3$ or $C_4$ plants to $PM_{2.5}$. The analyses were conducted using R-4.1.1[42].

## Results

### $δ^{13}C$ and $Δ^{14}C$ of TC in $PM_{2.5}$.
Both $δ^{13}C$ and $Δ^{14}C$ values of TRF were not significantly different from those of SNU on the same dates (n = 11) (Fig. 2 and Table 1). In contrast, the $Δ^{14}C$ values of CRI were significantly lower than those of TRF on the same collection dates in fall and winter (n = 5 each), with the mean $Δ^{14}C$ values of CRI and TRF at − 444.3‰ and − 380.7‰, respectively (Table 1). The $δ^{13}C$ and $Δ^{14}C$ values of TC in $PM_{2.5}$ varied temporally (Table 1) Enriched $δ^{13}C$ and $Δ^{14}C$ values were observed in winter and spring, while, in summer, $δ^{13}C$ and $Δ^{14}C$ were significantly depleted than other seasons (Fig. S3 in Supplementary Information).

### Concentration of TC and $PM_{2.5}$.
A total of 47 $PM_{2.5}$ samples were collected during the study period (Table 1). The mean concentrations of TC in $PM_{2.5}$ were 5.0, 7.0, 8.2, and 9.7 µg C m$^{-3}$ at TRF, HUF, CRI, and SNU, respectively (Table 1). The mean concentration of TC in $PM_{2.5}$ at SNU was about two-fold higher than at TRF ($p < 0.05$) (Table 1). The seasonal variation of TC in $PM_{2.5}$ was relatively small in summer (Jun.–Aug.) and larger in winter (Dec.–Feb.) (Fig. S4 in Supplementary Information) and the concentration of TC in $PM_{2.5}$ in winter was approximately 1.5-fold higher than in summer ($p < 0.05$).

The mean annual concentrations of $PM_{2.5}$ observed by the β-ray absorption method were 22, 20, 22 µg m$^{-3}$, respectively, at the national $PM_{2.5}$ monitoring sites located near TRF, HUF&CRI, and SNU in 2020, which were about 0.3–6.6 km away from our sampling sites (Fig. 3a). The concentration of $PM_{2.5}$ was not significantly different among monitoring sites ($p > 0.1$) regardless of seasons (Fig. 3a). The contribution of TC to $PM_{2.5}$ near monitoring sites ranged from 7 to 45% at TRF, from 16 to 86% at HUF and CRI, and from 8 to 69% at SNU (Table 1). The contribution of TC to $PM_{2.5}$ was the highest in spring at TRF and SNU (Table 1; Fig. 3).

### Source apportionments.
The contribution of the three sources (fossil fuel, $C_4$ plants, and $C_3$ plants) to TC in $PM_{2.5}$ was calculated. The contribution of carbon derived from fossil fuel ranged from 21 to 73% (Fig. 3b,c), with an average of 46%, 46%, 51%, and 51% at TRF, HUF, CRI, and SNU, respectively, based on the MCMC-Bayesian model (Table 2). The relative contribution of carbon from fossil fuel to TC in $PM_{2.5}$ was higher in summer than in winter at TRF and SNU (Table 2), which was expected from the depleted $δ^{13}C$ and $Δ^{14}C$ levels in summer (Fig. S3c in Supplementary Information).

The mean contributions of carbon from $C_4$ plants to TC in $PM_{2.5}$ were 19%, 17%, 21%, and 21% at TRF, HUF, CRI, and SNU, respectively (Table 2). The largest contribution of $C_4$ plants to TC in $PM_{2.5}$ was 42% and 55% for TRF and SNU, respectively, observed on April 10, 2020. A relatively lower contribution of $C_4$ plants was observed in summer (10% at TRF and 15% at SNU) compared with the other seasons (Table 2; Fig. 3b,c).

The mean contributions of carbon from $C_3$ plants to TC in $PM_{2.5}$ were 35%, 38%, 31%, and 27% at TRF, HUF, CRI, and SNU, respectively (Table 2). The highest contribution of $C_3$ plants to TC in $PM_{2.5}$ was observed in spring

| | Fossil fuel | $C_4$ plants | $C_3$ plants |
|---|---|---|---|
| **TRF** | | | |
| Spring (Mar.–May) | 1.5 ± 0.3 (29) | 1.2 ± 0.9 (22) | 2.5 ± 0.6 (49) |
| Summer (Jun.–Aug.) | 2.1 ± 0.5 (52) | 0.4 ± 0.1 (10) | 1.8 ± 1.2 (38) |
| Fall (Sep.–Nov.) | 1.7 ± 0.3 (44) | 0.4 ± 0.1 (12) | 1.9 ± 0.6 (44) |
| Winter (Dec.–Feb.) | 2.7 ± 0.8 (44) | 1.2 ± 0.4 (19) | 2.3 ± 1.1 (37) |
| Total | 2.1 ± 0.7 (46) | 0.8 ± 0.6 (19) | 2.1 ± 1.0 (35) |
| **HUF** | | | |
| Fall (10/13/2020) | 2.4 (44) | 0.8 (15) | 2.2 (41) |
| Winter (02/20/2020) | 4.2 (48) | 1.6 (18) | 2.9 (34) |
| Total | 3.3 ± 0.9 (46) | 1.2 ± 0.4 (17) | 2.6 ± 0.3 (38) |
| **CRI** | | | |
| Fall (10/14–16/2020) | 4.9 ± 0.6 (51) | 1.7 ± 0.3 (18) | 2.9 ± 0.4 (31) |
| Winter (02/21–24/2020) | 3.6 ± 0.5 (51) | 1.5 ± 0.5 (21) | 1.9 ± 0.3 (28) |
| Total | 4.2 ± 0.9 (51) | 1.6 ± 0.4 (21) | 2.4 ± 0.6 (29) |
| **SNU** | | | |
| Spring (Mar.–May) | 4.4 ± 1.8 (43) | 3.0 ± 2.7 (25) | 3.3 ± 1.9 (32) |
| Summer (Jun.–Aug.) | 3.5 ± 1.3 (62) | 1.0 ± 0.5 (15) | 1.5 ± 0.8 (24) |
| Fall (Sep.–Nov.) | 2.5 ± 0.5 (56) | 0.8 ± 0.4 (20) | 1.1 ± 0.2 (24) |
| Winter (Dec.–Feb.) | 6.1 ± 1.9 (43) | 5.3 ± 2.9 (32) | 3.5 ± 1.6 (25) |
| Total | 4.3 ± 0.01 (51) | 2.7 ± 0.01 (21) | 2.6 ± 0.01 (27) |

**Table 2.** The means and the standard deviations of the concentration (µg C m$^{-3}$) of each source. The mean relative contribution (%) of each source to carbonaceous component of $PM_{2.5}$ is in parentheses.

(49% at TRF and 32% at SNU), while in winter, the carbon contributions were 37, 34, 28, and 25% at TRF, HUF, CRI, and SNU, respectively (Table 2; Fig. 3b,c).

The concentration of TC in $PM_{2.5}$ from each source was calculated by multiplying the concentration of TC with the individual contribution. The mean concentration of TC in $PM_{2.5}$ derived from $C_3$ plants was 2.1 µg C m$^{-3}$ (range: 0.7–4.2 µg C m$^{-3}$) at TRF, and 2.6 µg C m$^{-3}$ (range 0.5–6.5 µg C m$^{-3}$) at SNU. Although the concentration of TC in $PM_{2.5}$ was about two-fold higher in SNU than in TRF (Table 1), the concentration of TC in $PM_{2.5}$ derived from $C_3$ plants was similar in the urban area and the pine forest (Table 2; Fig. 3b,c). In contrast, the mean concentration of TC in $PM_{2.5}$ derived from fossil fuel was 2.1 (range: 1.1–4.2 µg C m$^{-3}$) at TRF and 4.3 (range: 2.0–8.4 µg C m$^{-3}$) at SNU. The concentration of TC in $PM_{2.5}$ derived from $C_4$ plants ranged from 0.2 to 2.8 with an average of 0.8 µg C m$^{-3}$ at TRF, and ranged from 0.1 to 9.1 µg C m$^{-3}$ with an average of 2.7 µg C m$^{-3}$ at SNU (Table 2; Fig. 3b,c).
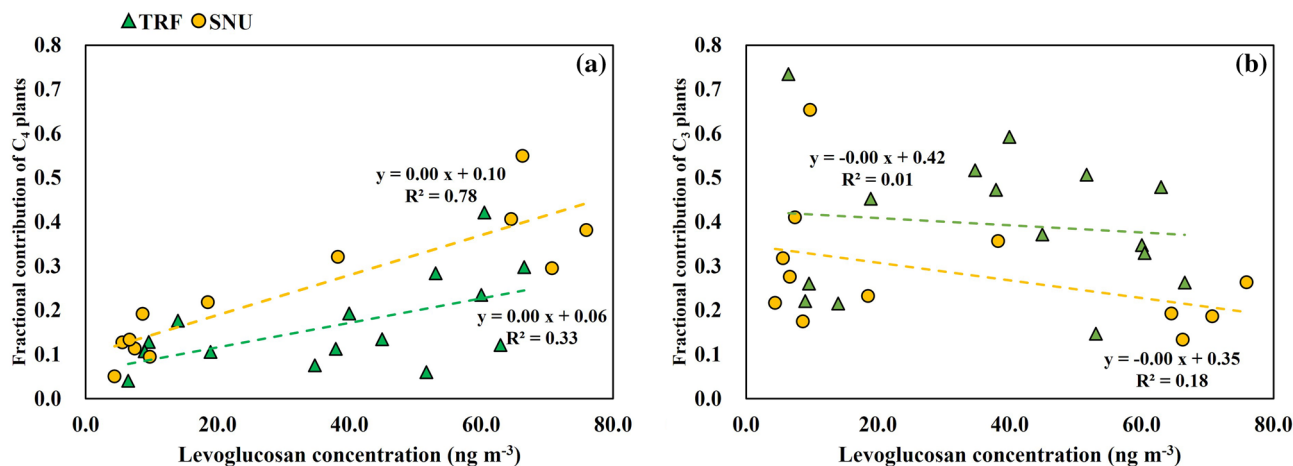
**Levoglucosan concentration.** The mean concentrations of levoglucosan were 39.8, 8.3, 34.6, and 57.5 ng m$^{-3}$ in spring, summer, fall, and winter, respectively, at TRF (Fig. 3d), whereas those at SNU were 30.4, 6.2, 12.6, and 70.4 ng m$^{-3}$, respectively (Fig. 3d). There was a positive correlation between the concentration of levoglucosan and fractional contribution of $C_4$ plants (Fig. 4a).

## Discussion

Many studies have demonstrated that $PM_{2.5}$ can be removed by trees[6,8–10], which leads to urban forest expansion. However, $PM_{2.5}$ can be indirectly produced by BVOCs emitted by plants[14,43,44]. $PM_{2.5}$ can also be directly produced by fossil fuel or biomass burning. These contrasting views question of their relative importance in the formation of $PM_{2.5}$. Although some studies on TC in $PM_{2.5}$ have been conducted in East Asia, typically in urban area, they used only $\delta^{13}C$ (not including $\Delta^{14}C$), different kind of dual isotopes ($\delta^{13}C$ and $\delta^{15}N$), or only during a limited season not over an entire year[34,35]. In contrast, this is the first study, to our knowledge, which investigated changes of $\delta^{13}C$ and $\Delta^{14}C$ of $PM_{2.5}$ over an entire year inside the forest and the urban areas in South Korea.

A review of $PM_{2.5}$ sources based on $^{14}C$ analysis demonstrated that the proportion of carbon sources except fossil fuels (i.e., total carbon minus carbon derived from fossil fuel) generally exceeded 30% of TC in PM collected even in urban locations[45]. If BVOCs derived from trees strongly contribute to the formation of $PM_{2.5}$, the $PM_{2.5}$ collected inside a forest would yield higher $\Delta^{14}C$ than in urban areas. In other words, as the portion of fossil carbon increases, $\Delta^{14}C$ will decrease. TC in $PM_{2.5}$ collected in the forest (TRF) and urban areas (SNU) had depleted $\Delta^{14}C$, indicating the relative contribution of fossil carbon is constantly high (Table 2 and Fig. 2). The similar sources of $PM_{2.5}$ in the forest and urban areas (Table 2 and Fig. 2) have been shown even during summer when the emission of BVOCs was the highest[46,47], or during spring when the concentrations of pollen were the highest[48] (Fig. S3 in Supplementary Information). This suggests that biogenic emission of plants could be a less important source of $PM_{2.5}$ even during summer. The $\Delta^{14}C$ values of $PM_{2.5}$ were also similar between TRF and HUF. CRI is located next to major traffic roads (Fig. 1), where direct input of $PM_{2.5}$ by vehicles could lower $\Delta^{14}C$. These results imply that trees can produce biogenic $PM_{2.5}$, but most of $PM_{2.5}$ within the forests or urban green spaces are likely to be transported from the outside.

Despite similar sources, the TC concentration in $PM_{2.5}$ at TRF was two-fold lower than at SNU (Table 1). Considering the similar concentrations of $PM_{2.5}$ at the monitoring sites which are located outside of forest (Fig. 3a), the lower concentrations of TC at TRF suggest that pine forests may reduce $PM_{2.5}$ transported from the outside. The ratio of fossil carbon to the total mass of $PM_{2.5}$ can be roughly calculated by multiplying the proportion of TC in $PM_{2.5}$ by the proportion of fossil carbon in TC. Since ~30% of $PM_{2.5}$ was carbonaceous material in general ("TC in $PM_{2.5}$ (%)" in Table 1)[19,45], and ~50% of the carbonaceous material was derived from fossil fuel (Table 2), ~15% of $PM_{2.5}$ (i.e., $0.3 \times 0.5 = 0.15$) is derived from fossil carbon. Although 15% appears small, the



**Figure 4.** The correlation between the concentration of levoglucosan and the fractional contribution of (**a**) $C_4$ plants, and (**b**) $C_3$ plants.

majority of the $PM_{2.5}$ is still attributable to the other aerosols, such as sulfur oxides and nitrogen oxides, derived from fossil fuel burning[27,28].

The remaining portions, ~ 50% of TC in $PM_{2.5}$ were attributed to the non-fossil fuels. A previous study conducted at TRF during the growing season (Aug.–Oct., 2014) showed approximately 76% of TC was from non-fossil sources[35]. We further attributed the non-fossil sources of TC in $PM_{2.5}$ to $C_3$ plants- (~ 30%) and $C_4$ plants-derived carbon (~ 20%) (Table 2), which was calculated over entire seasons including winter when the concentration of $PM_{2.5}$ was the largest. The range of $\delta^{13}C$ of marine aerosols could be in those between $C_3$ plants and $C_4$ plants[40,49]. Both $C_4$ plants and marine aerosols could be selected as an end member[28,40]. However, we have selected $C_4$ plants instead of marine aerosols as an endmember because of the variation of the concentration of levoglucosan (Fig. 3d). Levoglucosan is a tracer of biomass burning and thus cannot be an important component of marine aerosols[50]. The concentration of levoglucosan demonstrated clear seasonal variation, with the largest value up to 75.91 ng m$^{-3}$ observed during winter, followed by fall and spring, and the lowest during summer (Fig. 3d). This seasonal variation has been observed in major cities in the East Asia[26,51–54].

The concentration of levoglucosan was positively correlated with fractional contribution of $C_4$ plants (up to $R^2 = 0.78$, $p < 0.05$ in Fig. 4a), but not correlated with fractional contribution of $C_3$ plants (Fig. 4b). This indicates that the higher concentration of levoglucosan, especially in winter was likely due to the burning of $C_4$ plants (e.g., corn residues). The biomass burning of $C_4$ plants has been widely considered as one of the sources of TC in $PM_{2.5}$ because of the enriched $\delta^{13}C$ and the high concentration of levoglucosan during winter[26,34,55]. The enriched $\Delta^{14}C$ and $\delta^{13}C$ as well as the highest concentration of levoglucosan were also reported during winter in China[26–28].

Recent studies have demonstrated that the burning of corn residues accounted for up to 80% of the total agricultural waste burning in China[56–58]. China was the second-largest producer of corn with 23% of the global corn yield in the marketing year (Sep., 2019–Aug. 2020), following the U.S. very closely (https://www.fas.usda.gov/data/world-agricultural-production). In contrast, corn production in South Korea is substantially lower than in China. It has been also reported that the burning of corn residues was ~ 10% of the total agricultural waste burning in several rural areas of South Korea[59], although agricultural waste burning over the entire South Korea is rarely reported. Since northwesterly winds around Korea are predominant during winter as the Siberian High (i.e., Siberian Anticyclone) develops ([60]; Fig. S5 in Supplementary Information), TC derived from $C_4$ biomass burning could be not only generated within South Korea but also transported from North Korea and/or China[61,62].

Su et al.[63] quantified the proportion of nine sources of $PM_{2.5}$ by using a multivariate factor analysis in the western urban area of Shenzhen, China in the fall (Sep.– Nov., 2019). Among them, the contribution of biomass burning to the total concentration of $PM_{2.5}$ was only 11%[61]. The results of dual carbon isotope and levoglucosan analyses in this study showed about 20% of the carbonaceous component of $PM_{2.5}$ might be derived from the burning of $C_4$ plants. Considering TC accounted for ~ 30% of $PM_{2.5}$ [Table 1[19,45], the carbon derived from biomass burning of $C_4$ plants could contribute at least ~ 6% (i.e., 0.2 (above 20%) × 0.3 (above 30%) = 0.06) of the total $PM_{2.5}$, while inorganic materials can be attributed to another fraction of $PM_{2.5}$[64].

The carbon derived from $C_3$ plants was estimated at only ~ 9% of $PM_{2.5}$ in TRF and SNU, which can be attributed to biogenic emissions by trees or biomass burning of $C_3$ plants. The concentrations of TC derived from $C_3$ plants were similar at TRF and SNU, whereas the concentrations of TC derived from fossil-carbon and $C_4$ plants in the urban areas were about two-fold the levels at TRF (Table 2; Fig. 3b,c). Thus, biogenic emission of pines is not likely to be an important source of $PM_{2.5}$ in the forest, suggesting that trees act as a bio-filter of $PM_{2.5}$ in urban areas.

## Conclusions

We analyzed dual carbon isotope ratios and levoglucosan concentrations in a pine forest and in urban areas to provide source apportionment of TC in $PM_{2.5}$. The $\delta^{13}C$ and $\Delta^{14}C$ of TC in $PM_{2.5}$ indicated similar sources of carbon in $PM_{2.5}$ in the forest and urban areas, although the total concentration of TC in $PM_{2.5}$ was approximately two-fold lower in the forest than in urban areas. TC in $PM_{2.5}$ was predominantly affected by human activities such as fossil-fuel combustions and $C_4$ biomass burning rather than emissions from $C_3$ plants. These results suggest that strategies to reduce atmospheric $PM_{2.5}$ should focus on fossil fuel combustion and biomass burning instead of biogenic emissions from trees.

## Data availability

The data used to support the findings of this study are included within the article and its supplementary information files.

## References

1. Wang, Y., Zhang, R. & Saravanan, R. Asian pollution climatically modulates mid-latitude cyclones following hierarchical modelling and observational analysis. *Nat. Commun.* **5**, 3098. https://doi.org/10.1038/ncomms4098 (2014).
2. Xing, Y. F., Xu, Y. H., Shi, M. H. & Lian, Y. X. The impact of $PM_{2.5}$ on the human respiratory system. *Thorac. Dis.* **8**(1), E69. https://doi.org/10.3978/j.issn.2072-1439.2016.01.19 (2016).
3. Kim, Y., Yi, S. M. & Heo, J. Fifteen-year trends in carbon species and $PM_{2.5}$ in Seoul South Korea (2003–2017). *Chemosphere* **261**, 127750. https://doi.org/10.1016/j.chemosphere.2020.127750 (2020).
4. Hong, C. *et al.* Impacts of climate change on future air quality and human health in China. *Proc. Natl. Acad. Sci. U.S.A.* **116**(35), 17193–17200 (2019).
5. Seo, J. *et al.* Effects of meteorology and emissions on urban air quality: a quantitative statistical approach to long-term records (1999–2016) in Seoul, South Korea. *Atmos. Chem. Phys.* **18**(21), 16121–16137 (2018).

6. Nowak, D. J., Hirabayashi, S., Bodine, A. & Greenfield, E. Tree and forest effects on air quality and human health in the United States. *Environ. Pollut.* **193**, 119–129 (2014).

7. Nguyen, T., Yu, X., Zhang, Z., Liu, M. & Liu, X. Relationship between types of urban forest and PM$_{2.5}$ capture at three growth stages of leaves. *J. Environ. Sci.* **27**, 33–41 (2015).

8. Nowak, D. J., Hirabayashi, S., Doyle, M., McGovern, M. & Pasher, J. Air pollution removal by urban forests in Canada and its effect on air quality and human health. *Urban For. Urban Green.* **29**, 40–48 (2018).

9. Zhu, C. *et al.* Effect of spatial heterogeneity of plant communities on air PM10 and PM25 in an urban forest park in Wuhan, China. *Urban For. Urban Green.* **46**, 126487. https://doi.org/10.1016/j.ufug.2019.126487 (2019).

10. Irga, P. J., Burchett, M. D. & Torpy, F. R. Does urban forestry have a quantitative effect on ambient air quality in an urban environment?. *Atmos. Environ.* **120**, 173–181 (2015).

11. Heidt, V. & Neef, M. *Ecology, Planning, and Management of Urban Forests* (Springer, 2008).

12. Korea Forest Service. *Second Master Plan (2018–2027) for urban forests* (Korea Forest Service, 2019) (**in Korean**).

13. Park, J. H. *et al.* Active atmosphere-ecosystem exchange of the vast majority of detected volatile organic compounds. *Science* **341**(6146), 643–647 (2013).

14. Ehn, M. *et al.* A large source of low-volatility secondary organic aerosol. *Nature* **506**(7489), 476–479 (2014).

15. Keywood, M., Guyes, H., Selleck, P. & Gillett, R. Quantification of secondary organic aerosol in an Australian urban location. *Environ. Chem.* **8**(2), 115–126 (2011).

16. Shrivastava, M. *et al.* Urban pollution greatly enhances formation of natural aerosols over the Amazon rainforest. *Nat. Commun.* **10**(1), 1–12 (2019).

17. de Sá, S. S. *et al.* Urban influence on the concentration and composition of submicron particulate matter in central Amazonia. *Atmos. Chem. Phys.* **18**(16), 12185–12206 (2018).

18. Lemire, K. R., Allen, D. T., Klouda, G. A. & Lewis, C. W. Fine particulate matter source attribution for Southeast Texas using $^{14}$C/$^{13}$C ratios. *J. Geophys. Res. Atmos.* **107**(D22), ACH-3 (2002).

19. Szidat, S. *et al.* Radiocarbon ($^{14}$C)-deduced biogenic and anthropogenic contributions to organic carbon (OC) of urban aerosols from Zürich, Switzerland. *Atmos. Environ.* **38**(24), 4035–4044 (2004).

20. Heal, M. R. *et al.* Application of $^{14}$C analyses to source apportionment of carbonaceous PM$_{2.5}$ in the UK. *Atmos. Environ.* **45**(14), 2341–2348 (2011).

21. Genberg, J. *et al.* Source apportionment of carbonaceous aerosol in southern Sweden. *Atmos. Chem. Phys.* **11**(22), 11387–11400 (2011).

22. Liu, D. *et al.* The use of levoglucosan and radiocarbon for source apportionment of PM$_{2.5}$ carbonaceous aerosols at a background site in East China. *Environ. Sci. Technol.* **47**(18), 10454–10461 (2013).

23. Szidat, S. *et al.* Contributions of fossil fuel, biomass-burning, and biogenic emissions to carbonaceous aerosols in Zurich as traced by $^{14}$C. *J. Geophys. Res. Atmos.* https://doi.org/10.1029/2005JD006590 (2006).

24. Puxbaum, H. *et al.* Levoglucosan levels at background sites in Europe for assessing the impact of biomass combustion on the European aerosol background. *Geophys. Res. Atmos.* https://doi.org/10.1029/2006JD008114 (2007).

25. Salma, I. *et al.* Source apportionment of carbonaceous chemical species to fossil fuel combustion biomass burning and biogenic emissions by a coupled radiocarbon–levoglucosan marker method. *Atmos. Chem. Phys.* **17**(22), 13767–13781 (2017).

26. Zhao, Z. *et al.* Stable carbon isotopes and levoglucosan for PM$_{2.5}$ elemental carbon source apportionments in the largest city of Northwest China. *Atmos. Environ.* **185**, 253–261 (2018).

27. Ni, H. *et al.* Source apportionment of carbonaceous aerosols in Xi'an, China: insights from a full year of measurements of radiocarbon and the stable isotope $^{13}$C. *Atmos. Chem. Phys.* **18**(22), 16363–16383 (2018).

28. Mo, Y. *et al.* Dual carbon isotope-based source apportionment and light absorption properties of water-soluble organic carbon in pm25 over China. *J. Geophys. Res. Atmos.* **126**(8), e2020JD033920. https://doi.org/10.1029/2020JD033920 (2021).

29. Monson, R. K., Edwards, G. E. & Ku, M. S. C3–C4 intermediate photosynthesis in plants. *Bioscience* **34**(9), 563–574 (1984).

30. O'Leary, M. H. Carbon isotope fractionation in plants. *Phytochemistry* **20**(4), 553–567 (1981).

31. Lee, H. *et al.* The resilience of the carbon cycles of temperate coniferous and broadleaved forests to drought. *For. Ecol. Manag.* **491**, 119178. https://doi.org/10.1016/j.foreco.2021.119178 (2021).

32. Kim, S. Y. *et al.* Impact of biogenic volatile organic compounds on ozone production at the Taehwa Research Forest near Seoul, South Korea. *Atmos. Environ.* **70**, 447–453 (2013).

33. Food and Agriculture Organization of the United Nations. *Global Forest Resources Assessment 2020: Terms and Definitions.* (Food and Agriculture Organization of the United Nations, 2018).

34. Kundu, S. & Kawamura, K. Seasonal variations of stable carbon isotopic composition of bulk aerosol carbon from Gosan site, Jeju Island in the East China Sea. *Atmos. Environ.* **94**, 316–322 (2014).

35. Lim, S. *et al.* Source signatures from combined isotopic analyses of PM$_{2.5}$ carbonaceous and nitrogen aerosols at the peri-urban Taehwa Research Forest, South Korea in summer and fall. *Sci. Total Environ.* **655**, 1505–1514 (2019).

36. Wang, X., Ge, T., Xu, C., Xue, Y. & Luo, C. Carbon isotopic ($^{14}$C and $^{13}$C) characterization of fossil-fuel derived dissolved organic carbon in wet precipitation in Shandong Province China. *J. Atmos. Chem.* **73**(2), 207–221 (2016).

37. Wei, X. *et al.* $^{14}$C as a tool for evaluating riverine POC sources and erosion of the Zhujiang (Pearl River) drainage basin South China. *Nucl. Instrum. Methods Phys. Res. B.* **268**(7–8), 1094–1097 (2010).

38. Zhang, Y. L. *et al.* Fossil and nonfossil sources of organic and elemental carbon aerosols in the outflow from Northeast China. *Environ. Sci. Technol.* **50**(12), 6284–6292 (2016).

39. Raymond, P. A. The composition and transport of organic carbon in rainfall: Insights from the natural ($^{13}$C and $^{14}$C) isotopes of carbon. *Geophys. Res. Lett.* **32**(14), 2879. https://doi.org/10.1029/2005GL022879 (2005).

40. Ceburnis, D. *et al.* Quantification of the carbonaceous matter origin in submicron marine aerosol by $^{13}$C and $^{14}$C isotope analysis. *Atmos. Chem. Phys.* **11**(16), 8593–8606 (2011).

41. Phillips, D. L. & Gregg, J. W. Source partitioning using stable isotopes: Coping with too many sources. *Oecologia* **136**(2), 261–269 (2003).

42. R Core Team. *R: A Language and Environment for Statistical Computing* (R Foundation for Statistical Computing, 2021). https://www.R-project.org/.

43. McFiggans, G. *et al.* Secondary organic aerosol reduced by mixture of atmospheric vapours. *Nature* **565**(7741), 587–593 (2019).

44. Watanabe, A. C., Stropoli, S. J. & Elrod, M. J. Assessing the potential mechanisms of isomerization reactions of isoprene epoxydiols on secondary organic aerosol. *Environ. Sci. Technol.* **52**(15), 8346–8354 (2018).

45. Heal, M. R. The application of carbon-14 analyses to the source apportionment of atmospheric carbonaceous particulate matter: A review. *Anal. Bioanal. Chem.* **406**(1), 81–98 (2014).

46. Spracklen, D. V. *et al.* Aerosol mass spectrometer constraint on the global secondary organic aerosol budget. *Atmos. Chem. Phys.* **11**(23), 12109–12136 (2011).

47. Son, Y. S., Kim, K. J., Jung, I. H., Lee, S. J. & Kim, J. C. Seasonal variations and emission fluxes of monoterpene emitted from coniferous trees in East Asia: Focused on Pinus rigida and Pinus koraiensis. *J. Atmos. Chem.* **72**(1), 27–41 (2015).

48. Rahman, A. *et al.* Influence of atmospheric PM$_{2.5}$, PM$_{10}$, O$_3$, CO, NO$_2$, SO$_2$, and meteorological factors on the concentration of airborne pollen in Guangzhou China. *Atmos. Environ.* **212**, 290–304 (2019).

10

49. Miyazaki, Y., Kawamura, K., Jung, J., Furutani, H. & Uematsu, M. Latitudinal distributions of organic nitrogen and organic carbon in marine aerosols over the western North Pacific. *Atmos. Chem. Phys.* **11**, 3037–3049 (2011).
50. Fu, P. Q., Kawamura, K., Chen, J., Charrière, B. & Sempere, R. Organic molecular composition of marine aerosols over the Arctic Ocean in summer: Contributions of primary emission and secondary aerosol formation. *Biogeosciences* **10**, 653–667 (2013).
51. Cheng, Y. *et al.* Biomass burning contribution to Beijing aerosol. *Atmos. Chem. Phys.* **13**, 7765–7781 (2013).
52. Choi, J. K., Heo, J. B., Ban, S. J., Yi, S. M. & Zoh, K. D. Chemical characteristics of $PM_{2.5}$ aerosol in Incheon, Korea. *Atmos. Environ.* **60**, 583–592 (2012).
53. Choi, N. R., Lee, S. P., Lee, J. Y., Jung, C. H. & Kim, Y. P. Speciation and source identification of organic compounds in $PM_{10}$ over Seoul, South Korea. *Chemosphere* **144**, 1589–1596 (2016).
54. Kim, H., Kim, J. Y., Jin, H. C., Lee, J. Y. & Lee, S. P. Seasonal variations in the light-absorbing properties of water-soluble and insoluble organic aerosols in Seoul, Korea. *Atmos. Environ.* **129**, 234–242 (2016).
55. Zhang, T. *et al.* Identification and estimation of the biomass burning contribution to Beijing aerosol using levoglucosan as a molecular marker. *Atmos. Environ.* **42**(29), 7013–7021 (2008).
56. Cui, S. *et al.* Spatial and temporal variations of open straw burning based on fire spots in northeast China from 2013 to 2017. *Atmos. Environ.* **244**, 117962. https://doi.org/10.1016/j.atmosenv.2020.117962 (2020).
57. Jin, Q., Ma, X., Wang, G., Yang, X. & Guo, F. Dynamics of major air pollutants from crop residue burning in mainland China, 2000–2014. *J. Environ. Sci.* **70**, 190–205 (2018).
58. Li, C. *et al.* Light absorption characteristics of carbonaceous aerosols in two remote stations of the southern fringe of the Tibetan Plateau, China. *Atmos. Environ.* **143**, 79–85 (2016).
59. Kim, D. Y., Choi, M.-A., Han, Y.-H. & Park, S.-K. A study on estimation of air pollutants emission from agricultural waste burning (in Korean with English abstract). *J. Korea Soc. Atmos. Environ.* **32**(2), 167–175 (2016).
60. Jhun, J. G. & Lee, E. J. A new East Asian winter monsoon index and associated characteristics of the winter monsoon. *J. Clim.* **17**(4), 711–726 (2004).
61. Heo, J. B., Hopke, P. K. & Yi, S. M. Source apportionment of $PM_{2.5}$ in Seoul Korea. *Atmos. Chem. Phys.* **9**(14), 4957–4971 (2009).
62. Park, Y. M. *et al.* Characterizing isotopic compositions of TC-C $NO_3^-$-N and $NH_4^+$-N in $PM_{2.5}$ in South Korea: Impact of China's winter heating. *Environ. Pollut.* **233**, 735–744 (2018).
63. Su, C. P. *et al.* Development and application of a mass closure $PM_{2.5}$ composition online monitoring system. *Atmos. Meas. Tech.* **13**(10), 5407–5422 (2020).
64. Xie, Y., Zhao, Y. & Xiao, H. Effects of secondary formation of inorganic ions and low molecular weight organic acids and biomass burning in regional pollution of $PM_{2.5}$ in Central China. *Atmos. Pollut. Res.* **13**(5), 101412 (2022).

## Acknowledgements

## Author contributions

J.Y.C.: Methodology, formal analysis, investigation, writing—original draft preparation, and writing—review & editing, visualization. K.L., S.C.L., E.J.L., K.J.Y, I.R., M.K.: Investigation, and writing—review & editing. J.A., S.M.Y., C.R.P.: Resources, and writing—review & editing. N.H.O.: Conceptualization, supervision, writing—original draft preparation, writing—review & editing, and funding acquisition.

## Competing interests

The authors declare no competing interests.

## Additional information

**Supplementary Information** The online version contains supplementary material available at https://doi.org/10.1038/s41598-023-32721-2.

**Correspondence** and requests for materials should be addressed to N.-H.O.

**Reprints and permissions information** is available at www.nature.com/reprints.

**Publisher's note** Springer Nature remains neutral with regard to jurisdictional claims in published maps and institutional affiliations.